Dynamic behaviour of railway track

In 1995, the Faculty of Civil Engineering of TU Delft completed a study on the behaviour of 'Paved-in light rail track constructions' [1]. Apart from investigating the different construction types, in-track measurements of quasi-static deflections under passing vehicles were conducted. These measurements aimed at estimating construction parameters to analyse the dynamic response in the vertical direction. Using an excitation hammer, dynamic responses were measured at a number of locations and these were compared with calculated values. This article discusses some of these results and provides the theoretical background.

By: Prof. Dr. Ir. C. Esveld, Ir. J. van 't Zand, Ir. P.N. Scheepmaker, Ir. A.S.J. Suiker
TU Delft, Faculty of Civil Engineering, The Netherlands.

Quasi-static analyses are often used when designing railway track structures. These mainly consist of calculating deflections under static train loads and multiplying the results by a safety factor. For curves, the deflections due to non-compensated lateral accelerations are superimposed. If the dynamic effects are also considered, the equation

$$K = \frac{d(mv)}{dt}$$

has to be applied. For constant mass this means the well-known formula: force equals mass times acceleration. The response x to an excitation F can either be calculated via convolution (Du Hamel Integral) in the time domain:

$$x(t) = \int_0^t F(\tau)h(t-\tau)d\tau$$

or via multiplication in the frequency domain according to:

$$X(f) = H(f)F(f)$$

The function h is called the unit impulse response function and H is referred to as the transfer function. Both are related via a Fourier transform as follows:

$$h = FT(H) \text{ and } H = FT^{-1}(h)$$

The wheel/rail forces, which act as dynamic loads on the track, follow from the interaction between vehicle and track. If the aim of the analysis is to investigate high-frequency phenomena in relation to loads due to imperfections in wheel and rail geometry, the P_1 and P_2 forces have to be considered, as shown in Fig. 1. The forces are described by the following equations [3]:

$$P_1 = Q_{st} + 2\alpha\, v \sqrt{\frac{k_H m_e}{1 + m_e/m_u}}$$

$$P_2 = Q_{st} + 2\alpha\, v \sqrt{\frac{m_u}{m_u + m_t}} \left[1 - \frac{c_t \pi}{4k_t\sqrt{m_u + m_t}}\right] \sqrt{k_t m_u}$$

in which:
2α = total dip angle, m_u = vehicle unsprung mass, m_t = rail mass per unit length, m_e = effective track mass, k_h = Hertzian spring stiffness, k_t = track stiffness, c_t = track damping, v = vehicle speed in m/s.

For low-frequency dynamics, the interaction follows from a vehicle-track interaction model, which is described in [3], [4] for example. The relationship between a train and the dynamic variations in track geometry can be described via a linear multiple-input single-output system. Each track geometry component has a specific contribution to, for instance, a wheel-rail force. These relationships can easily be formulated in the frequency domain with the help of transfer functions. The q inputs $X_j(s)$ produce the outputs $Y_i(s)$ via q linear systems according to:

$$Y_i(f) = \sum_{j=1}^{q} H_{ij}(f)\, X_j(f)$$

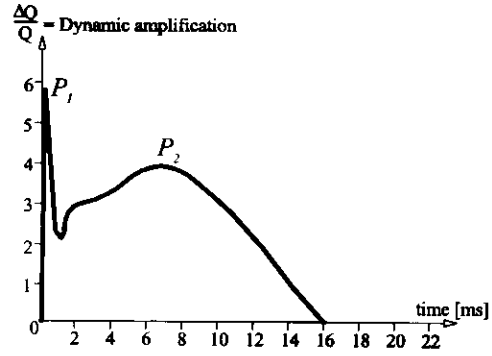

Fig. 1: Dynamic wheel load during passage over a weld

in which $H_{ij}(f)$ represents the transfer functions between input and output. All the records are complex valued, which means that there is a real part and an imaginary part, or equivalently a modulus and an argument (phase). The maximum response value per signal can be determined via a back transformation according to:

$$y_i(s) = \int_{-\infty}^{\infty} Y_i(f) e^{i2\pi fs} df$$

For a given force, the dynamic response can be estimated using a relatively simple model of an elastically-supported beam on a Winkler foundation. The differential equation for that beam can be described as follows:

$$EIy^{iv}(x,t) + m\ddot{y}(x,t) + c\dot{y}(x,t) + ky(x,t) = 0$$

With the boundary conditions:

$$EIy''(0,t) = 0.5Qe^{i2\pi ft}\ ;\ y'(0,t) = 0;\ y(\infty,t) = 0$$

the following solution for the transfer function is found:

$$H_r(f) = \frac{1}{2kL}\left\{\left[1 - \frac{f^2}{f_n^2}\right]^2 + 4\varsigma^2\frac{f^2}{f_n^2}\right\}^{\frac{3}{8}} e^{i\Phi}$$

$$\phi = -\frac{3}{4}\, a\tan\left(\frac{2\varsigma\frac{f}{f_n}}{1 - \frac{f^2}{f_n^2}}\right)$$

in which EI = bending stiffness, L = characteristic length, m = mass, k = stiffness, c = damping, ς = damping ratio.

Model used for analysing light rail track

Instead of working with analytical models it is often more convenient to use finite element models or discrete element models due to the flexibility in boundary shapes. The studies related to the project on light rail track dynamics described above were carried out using the TILLY discrete element program developed at TU Delft.

A dynamic analysis may consist of various levels of sophistication, varying from a quasi-static approach to the determination of total stresses under moving vehicles or complete trains. As a first step the TILLY analyses were used to determine the dynamic characteristics of the track, i.e. to analyse the susceptibility of the track to specific frequencies of the load spectrum generated by passing trains. Coincidence of excitation frequencies, either consisting of natural frequencies of rolling stock components, or frequencies induced by geometrical imperfections of wheel and rail, should be avoided.

In the study referred to in [1] a stratified track model was developed as shown in Fig. 2. The track structure, which is depicted on the left, can be described as follows: in the longitudinal direction of the track, prefabricated concrete slabs of 18 cm thickness are used as a substructure and supported by layers of asphalt and soil. Nikex block rails are positioned in grooves of the concrete slabs and are continuously supported by an elastic layer.

In the track model, shown on the right, the rail is divided in small discrete elements and, at intervals of 10 cm, supported by visco-elastic elements, characterised by one discrete spring and damper per support, mounted between rail and slab. The concrete slab and supporting layers are likewise split up in discrete elements.

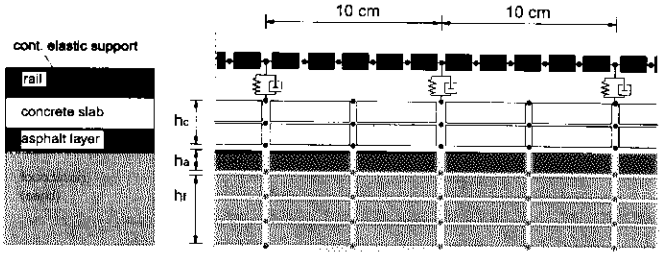

Fig. 2: Track model to describe Nikex construction

Rail (Nikex profile)	mass	52.75 kg/m
	I	261.637e-8 m^4
	A	6720e-6 m^2
Rubber supports	stiffness	100e6 N/m/m
	damping	30e3 Ns/m/m
Concrete slab	height	0.18 m
	E	3e10 N/m^2
	ν	0.45
	ρ	2400 N/m^3
Asphalt	height	0.12 m
	E	4e9 N/m^2
	ν	0.45
	ρ	2300 N/m^3
Foundation (three sand layers)	height	0.12 m each
	E	2e8 N/m^2
	ν	0.45
	ρ	1820 N/m^3

Properties of Nikex construction

The dynamic analysis of this Nikex construction consisted of determining the response due to a pulse-shaped load. The time function of load and displacement, depicted in Fig. 3, were Fourier transformed with the help of MATLAB to produce the transfer function as a function of frequency, which is displayed in Fig. 4. The frequency response peak at about 200 Hz is due to the natural rail vibration on the rubber support.

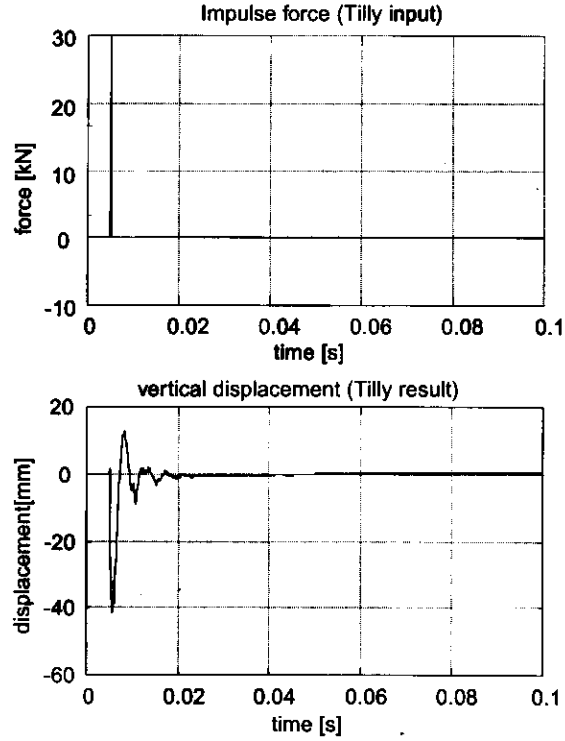

Fig. 3: Impulse force and displacement response of Nikex construction determined with TILLY

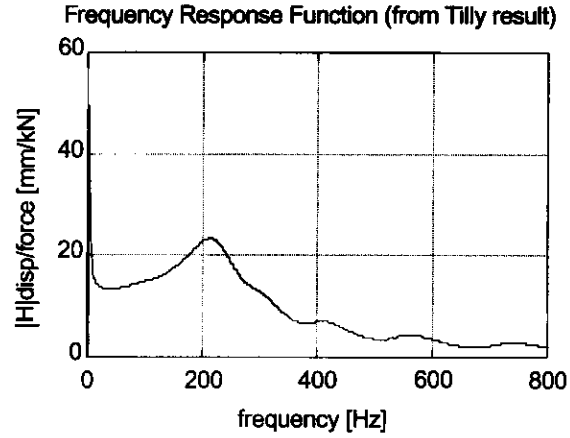

Fig. 4: Transfer function for Nikex construction determined with FFT from TILLY

Moving load passing a stiffness transition zone

Various studies on dynamic behaviour of railway track are presently being carried out at TU Delft. One of them is dealing with stresses due to a moving load passing a stiffness transition zone in an elastic stratified half-space. The numerical analysis has been performed using the finite element program DIANA. Fig. 5 shows an example of a stiffness transition, modelled as a two-dimensional configuration. A superficial layer with a thickness of 10.5 m and a length of 90 m has a modulus of elasticity of $E = 25 \times 10^6$ N/m^2. The ambient formation is four times as stiff. The finite element model has been constructed of 4-noded linear plane stress elements (0.75×0.75 m), combined with a 2×2 Gauss integration scheme.

The continuous moving load, propagating at a speed of 30 m/s, is modelled as an assemblage of successive discrete pulses. In order to model a half-space situation properly, the wave energy of the arriving waves is absorbed at the model boundaries. The load initiation starts at a horizontal distance of 60 m from the left boundary. The semi-discrete equations of motion were integrated using a damped Newmark scheme, combined with a time-step of $\Delta t = 0.002$ seconds.

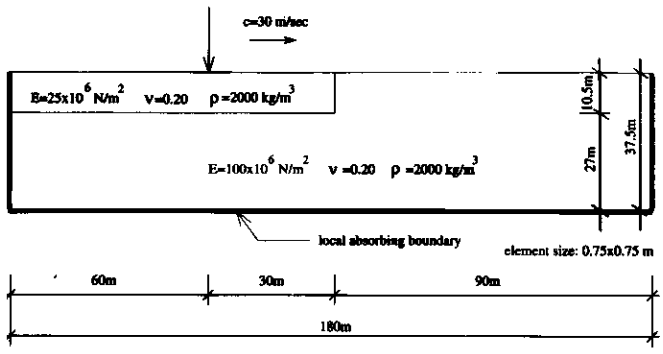

Fig. 5: Configuration of a moving load on a stratified half-space, containing a superficial layer with variable stiffness

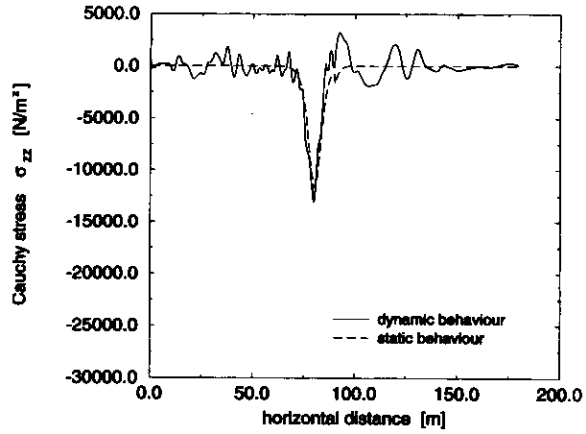

6a: After 20 m of load propagation (horizontal distance = 80 m)

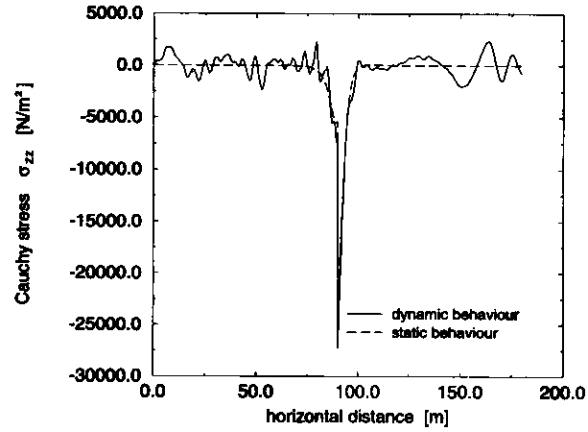

6b: After 30 m of load propagation (horizontal distance = 90 m)

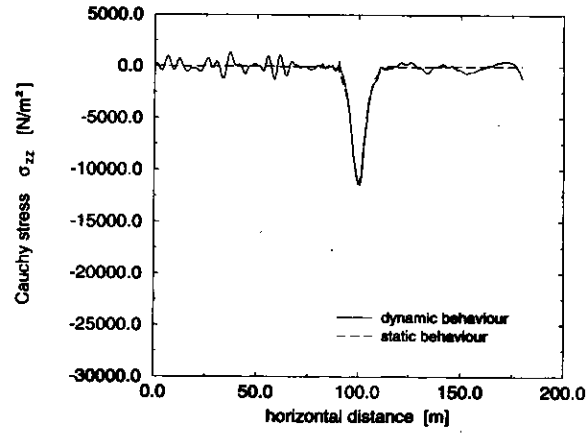

6c: After 40 m of load propagation (horizontal distance = 100 m)

Fig. 6: Vertical stress σ_{zz} at 5.84 m beneath the surface for various load distances

Fig. 6 shows the vertical stress σ_{zz} at 5.84 m beneath the surface, for various load distances. With respect to Fig. 6a, the load has propagated a distance of 20 m. It can be seen that the largest compression stress occurs right beneath the load. The oscillations in front of the load are due to Rayleigh surface waves, as a result of increasing the travelling speed from 0 m/s to 30 m/s. Under current material conditions the Rayleigh wave speed is higher than the load propagation speed (*subsonic speed range*) and thus its influence runs out of the domain considered after a certain time. For the soft material, with $E = 25 \times 10^6$ N/m^2, the Rayleigh wave speed is 65 m/s, whereas for the stiff material it is 131 m/s.

After the load has propagated over a distance of 30 m, it enters the vertical stiffness transition (Fig. 6b), at which a relatively large value of σ_{zz} is generated. This is caused by the fact that, according to the theory of elasticity, the strains in both materials have to be compatible at the material transition interface. The response behind the load seems coarse compared to the smoother response in front of the load. This is due to reflections at the layer interface in the first 90 m of the model.

Fig. 6c reveals that after 40 m of load propagation the influence of Rayleigh waves has almost vanished; the behaviour is nearly equivalent to the 'steady state' response of a homogeneous isotropic elastic half-space.

Dividing the maximum dynamic stress underneath the load by the corresponding static stress gives the dynamic amplification. After 20 m of load propagation (Fig. 6a) the dynamic amplification factor for the load propagation speed of 30 m/s equals 1.12. At the material interface (Fig. 6b) the largest amplification is reached (28%). On the soft layer the amplification factor falls back to 1.02.

Experiments

There are various methods of obtaining dynamic parameter values for use in dynamic track models. For instance, the signals from an instrumented track responding to passing rail vehicles can be measured. Such an approach was adopted in the measurements referred to in [1]. In this research, the rail displacements were measured using an optical system, to collect quasi-static track parameters, some results of which are given in Fig. 7.

Fig. 7a shows a typical vertical rail displacement of, in this case, a continuously-supported block rail (Nikex track). This measurement was sampled at 204.8 Hz, which allows the low-frequency content to be studied up to about 100 Hz.

As can be seen in Fig. 7b, the autospectrum of the displacement signal shows some distinct peaks. Taking into account the wheel configuration of the light rail vehicle (GTL-8) and the running speed of 26 km/h, the two large peaks are identified as mean bogie distance (about 1 Hz) and axle spacing in a bogie (3.8 Hz) respectively. However, the vibration energy of the passing vehicle is very dominant and tends to obscure the location of natural frequencies of the track system in the graph.

To determine the dynamic parameters of the track system itself a modal analysis with a well-defined measurable dynamic load is necessary. A very convenient way to excite the system is to use an instrumented excitation hammer, which generates a short load pulse at a certain point of the test structure. The output consists of one or more response signals, which are mostly acceleration signals. Based on an assumed mathematical dynamic model, curve fitting is carried out in the frequency domain. This technique is also employed by TU Delft to assess dynamic stiffness and damping of rail pads in the laboratory [2].

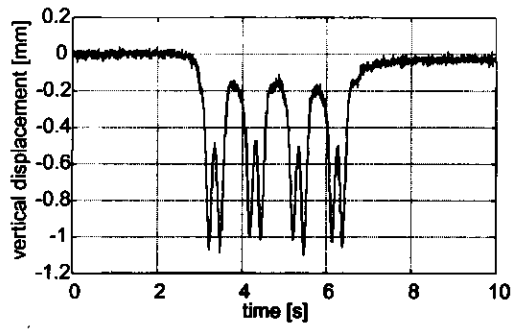

7a: Measured displacement signal

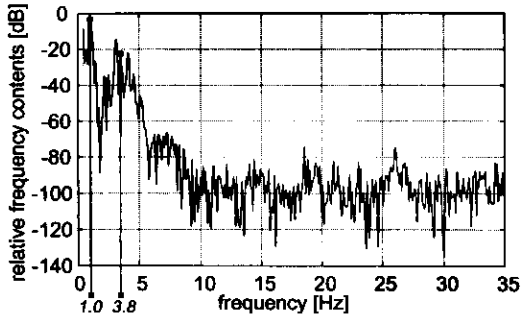

7b: Autospectrum of measured displacement signal

Fig. 7: Vertical rail displacement and autospectrum due to a passing light rail vehicle

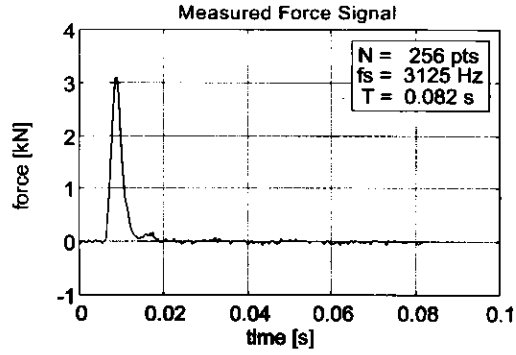

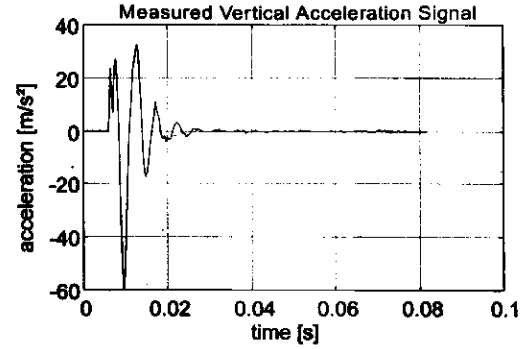

Fig. 8: Pulse load and rail vertical response using a heavy excitation hammer

Recently, this technique was generalised to enable the modal testing of more complicated track components like complete rail-sleeper assemblies, or even full-scale railway tracks. In this case a heavy excitation hammer is used to transmit sufficient energy into the track to be tested. Fig. 8 shows measurement results, consisting of the input (load pulse) and the output (vertical acceleration) measured near the load application point. The track tested was the same Nikex track as referred to earlier. Fig. 9 shows the averaged frequency response function (inertance function) and the accompanying coherence function based on seven repeated hammer excitations. The frequency of the peak value at about 200 Hz corresponds fairly well with the theoretical value presented in Fig. 4, produced with the TILLY model. The large peak at about 400 Hz is due to lateral rotation of the rail section.

Experience gained so far reveals the excitation hammer to be a versatile tool for checking the dynamic behaviour of railway track, provided that appropriate precautions are taken regarding data acquisition and data analysis. Improvements are being developed by TU Delft to widen the scope of such applications. For instance, the number of accelerometers will be increased to enable the study of multiple degree-of-freedom systems. A two-degree-of-freedom model is implemented in the curve fitting procedure to determine the dynamic parameters of two-layer track systems.

Concluding remarks

When railway designs are approaching system limits it is natural that full consideration be given to the dynamic behaviour of the track and also to the interaction between vehicle and track. This is particularly true for high-speed train operation, but the significance of these phenomena to heavy haul should not be underestimated either. In the light rail sector, dynamics are particularly relevant to noise and vibration reduction. TU Delft is currently carrying out the following research projects:

— wave propagation due to high-speed train operation;
— vibration analysis of railway track;
— dynamic amplification due to stiffness transitions;
— vehicle/track interaction;
— in-situ measurement of dynamic track response;
— laboratory tests on track components.

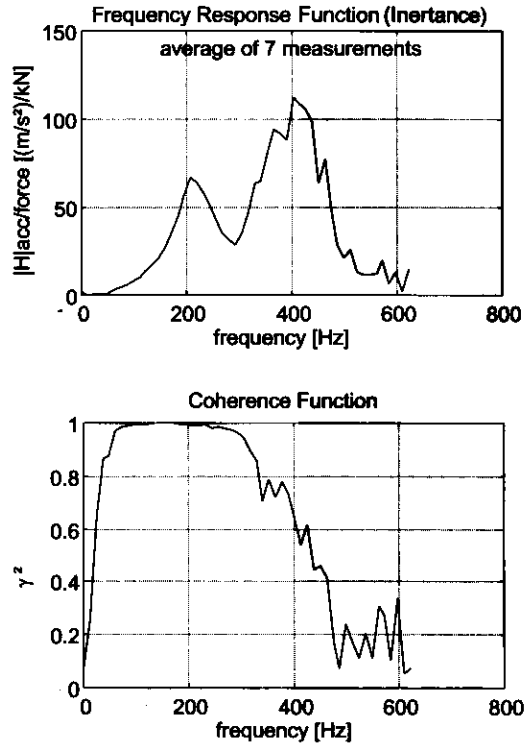

Fig. 9: Inertance and coherence function

References

[1] Scheepmaker P.N., Zand J. van 't: 'Paved-in light rail track constructions', Rail Engineering International, Edition 1994, Number 3, pp. 9-12.

[2] Zand J. van 't: 'Assessment of dynamic characteristics of rail pads', Rail Engineering International, Edition 1994, Number 4, pp. 15-17.

[3] Jenkins H.H. et al: 'The effect of track and vehicle parameters on wheel/rail vertical dynamic forces', Rail Engineering Journal, January 1974, pp.2-16.

[4] Esveld C.: 'Modern Railway Track', MRT-Productions, 1989 (ISBN 90-800 324-1-7).